Shallow-donor impurities in indium selenide investigated by means of far-infrared spectroscopy

J. Martinez-Pastor and A. Segura
Departamento Física Aplicada, Universitat de València, 46100 Burjassot, Valencia, Spain

C. Julien
Laboratoire de Physique des Solides, Université Pierre et Marie Curie, 4 place Jussieu, 75252 Paris, CEDEX 05, France

A. Chevy
Laboratoire de Physique des Milieux Condensés, Université Pierre et Marie Curie, 4 place Jussieu, 75252 Paris, CEDEX 05, France

(Received 29 October 1991; revised manuscript received 16 March 1992)

Shallow impurities in n-type indium selenide (InSe) have been investigated by means of Fourier-transform spectroscopy in the far-infrared region. Three electric dipole transitions have been identified: $1s$-$2p_{\pm}$, $1s$-$2p_0$, and $1s$-$3p_{\pm}$, corresponding to electrons bound to native donors and tin-, silicon-, and chlorine-related donors, whose ionization energies (17.6, 18.1, 18.8, and 19 meV, respectively) have been determined through the Guerlach-Pollmann model. That model was also used to calculate the oscillator strengths of those dipole transitions, and then to estimate the shallow-donor concentrations in each sample. Native donors turn out to be the most hydrogenic ones, and the energies of their related transitions are used to determine a more accurate value of the low-frequency dielectric-constant product. An absorption line is observed in the low-energy side of the spectra (80 cm^{-1}) for samples with a donor concentration higher than 10^{15} cm^{-3}, which is attributed to impurity pairing. A mechanism is proposed to explain the large value of the full width at half maximum associated with the $1s$-$2p_{\pm}$ absorption line (≈ 6.6 cm^{-1} in the purest samples): Longitudinal-acoustic phonons polarized parallel to the c axis create dielectric-constant waves that modulate the dipole transition energies of shallow donors. In highly doped samples, compensating acceptors give rise to internal electric fields that largely broaden the absorption lines.

I. INTRODUCTION

Among the layered semiconductors indium selenide (InSe) is the only one in which several shallow donors have been detected and characterized. Unintentionally doped InSe, prepared by the Bridgman method, is always n type, with electron concentrations ranging from 10^{13} to 10^{15} cm^{-3}.[1-5] The native donor is shallow, with an ionization energy of 18.5 meV, as determined from Hall effect (HE) results.[4] The related $1s$-$2p_{\pm}$ electronic transition has also been observed, at an energy of 12.7 meV, by far-infrared (FIR) absorption.[6] This shallow level has been attributed to interstitial indium atoms[4] as well as to selenium vacancies.[7]

As regards substitutional impurities, tin (Sn) has been shown to create a shallow donor in InSe, with an ionization energy of 22 meV, as obtained from HE measurements.[10] Tin-related deep donor and compensating accepters in InSe have also been detected and studied through HE and deep level transient spectroscopy.[8-11]

As a uniaxial crystal with nondegenerate conduction band,[12] InSe is a good system to test models for shallow donors. In recent years, InSe, as well as the related compound gallium selenide (GaSe), were used to test models for anisotropic excitons,[13,14] but, obviously, only the s states that give rise to structures in the absorption edge were studied.

In this work we report a systematic investigation of shallow-donor impurities in InSe, by means of FIR absorption (Sec. III). These results are discussed in Sec IV in the framework of the Gerlach-Pollmann model for uniaxial crystals.[15]

II. EXPERIMENT

The InSe crystals studied in this work were grown using the Bridgman method, from a nonstoichoimetric $In_{1.05}Se_{0.95}$ melt.[3,16] In this work, we use samples from ingots doped with different amounts of group-IV elements (Si, Ge, Sn, and Pb), group-VII (Cl), and isoelectronic impurities (Ga, S). Doping agents were introduced into the polycrystalline powder as compounds like $InCl_3$, SnSe, etc. The impurity concentration in the melt must be as high as 1%, in order to get free electron concentrations of the order of 10^{17} cm^{-3}. Nevertheless, the impurity segregation coefficients are very high in InSe and only a very low proportion of those impurities remain in the crystal, the rest being rejected to the end of the crystal with the In excess. Some impurities remain in the crystal and create deep levels or not electrically active centers. From the point of view of this study that is irrelevant, as they do not give rise to electronic absorption peaks in the FIR region. Table I gives the average HE carrier concentrations at room temperature for the ingots studied in the present work, which give a first indication of the shallow-donor concentration.

Most samples were cleaved along the plane perpendicular to the c axis with a razor blade, and cut into paral-

TABLE I. Hall effect concentration measured in the ingots used in this work.

Ingot	Doping agent	n_H (300 K) (10^{15} cm^{-3})
ID	Ga	1–3
SiD-1	Si	4–10
SnD-1	Sn	1–3
SnD-2	Sn	3–7
SnD-3	Sn	20–40
SnD-4	Sn	80–100
ClD	Cl	1–2
PbD	Pb	0.1 (p-type)

lelepipeds with convenient thickness (listed in Table II) and 5×5 mm^2 in size. In this configuration, the polarization of the light is always perpendicular to the c axis for normal incidence. Other samples were cut along the c axis with a diamond saw, in order to achieve optical quality faces, parallel to that direction. Thus we could study the effect of light polarization with respect to the c axis. On the other hand, annealing of several samples at 300 °C was also carried out in order to study its effect on shallow-donor concentration (recleaving of the original samples was necessary for avoiding overabsorption).

Fourier-transform spectroscopy in the FIR region has been carried out using a BRUKER computer-assisted system. Low temperatures were achieved by means of an OXFORD cryogenic system, composed of an optical cryostat, temperature controller, vacuum pump, and liquid-helium flux controller.

III. RESULTS

In order to clearly identify shallow-donor-related peaks, the intrinsic absorption spectrum of InSe must first be studied. N-type samples with electron concentra-

TABLE II. Best fitting parameters: line position (first column), FWHM (second column), and integrated absorption intensity (third column), deduced from the observed absorption lines in the different ingots. The donor concentrations in each sample are listed in the fourth column (calculated from the integrated absorption intensity of P_n lines and corresponding oscillator strength). The sample thicknesses are listed in the fifth column.

Sample	Line	σ_{max} (cm^{-1})	Γ (cm^{-1})	I (cm^{-2})	N_D (cm^{-3})	Thickness (μm)
ID	P_1	102.5	6.6	150	1.54×10^{14}	480
ID (annealed)	A	76.5	19.5	270		280
	P_1	103.5	8.3	890	9.13×10^{14}	
	B_1	125.1	21.5	810		
SnD-1	P_1	103.0	8.4	150	1.57×10^{14}	500
	P_2	112.1	12.0	120	1.44×10^{14}	
SnD-1 (annealed)	A	77.8	16.4	940		165
	P_1	102.9	16.6	3 900	4.14×10^{15}	
	P_2	114.1	13.1	1 600	1.89×10^{15}	
	B_1	127.0				
SnD-2	P_1	103.7	9.8	400	4.11×10^{14}	390
	P_2	112.0	9.3	770	8.94×10^{14}	
SnD-2 (annealed[a])	P_1	104.1	6.6	520	5.30×10^{14}	140
	P_2	109.5	8.2	2 160	2.52×10^{15}	
	B_2	132.0	18.6	1 130		
SnD-3[b]	A	77.7	32	310		200
	P_2	113.6	24.2	4 700	5.47×10^{15}	
	B_2	135.0	24.4	1 000		
SnD-4[b]	A	78.0	33	16 400		40
	P_2	112.2	31	30 000	3.49×10^{16}	
	B_2	135.3	40	9 100		
SiD	A[c]	80.0	14.0	45		500
	P_3	105.9	9.6	1 200	4.0×10^{15}	200
	B_3	129.7	16.9	300		
ClD	P_1	102.8	12.6	35	3.6×10^{13}	850
	P_4	113.7	13.6	100	1.2×10^{14}	
SnD-1 (pol. $\perp c$)	P_1	101.7	15.6	190	2.3×10^{14}	1000
	P_2	111.3	17.6	360	4.3×10^{14}	
SnD-1 (pol. $\parallel c$)	C_1	110.0	13.0	140	1.7×10^{14}	1000
	C_2	124.3	20.8	250	3.0×10^{14}	
		1	2	3	4	5

[a]Sample measured a day after the annealing.
[b]In these samples the concentration should correspond to N_D-N_A instead of N_D.
[c]Parameters obtained from a thicker sample.

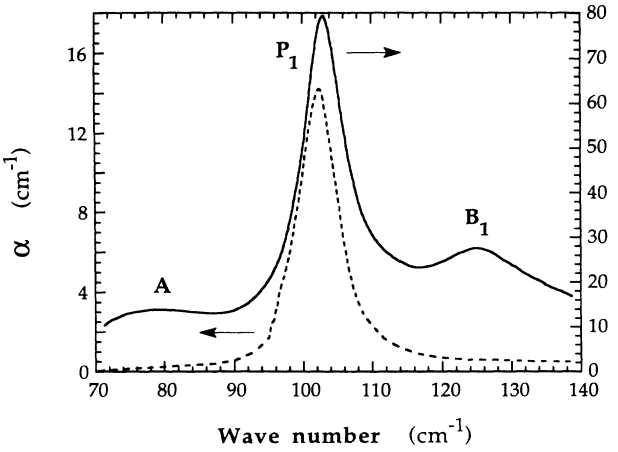

FIG. 1. Impurity absorption coefficient at 5 K for a sample from the nondoped ingot (ID), before (dotted line) and after annealing (continuous line).

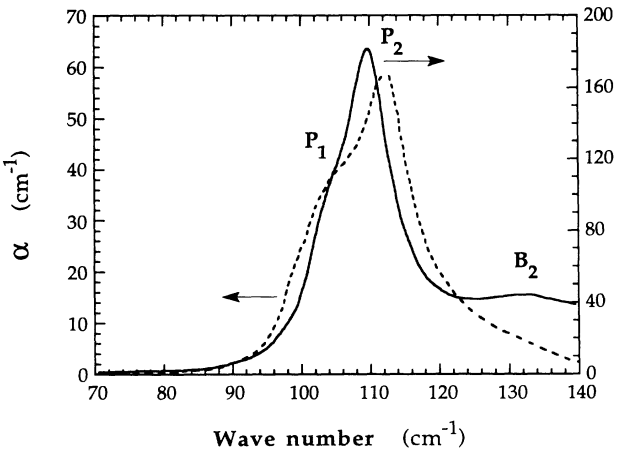

FIG. 3. Impurity absorption coefficient at 5 K for a sample from the SnD-2 ingot, before (dotted line) and after annealing (continuous line).

tions lower than 10^{14} cm^{-3} (at room temperature) and p-type samples have the same FIR absorption spectra, where only phonon absorption peaks are observed at 4.2 K. Between 170 and 220 cm^{-1} the crystal is opaque due to polar TO-phonon absorption.[17] Many multiphonon absorption lines appear between 220 and 450 cm^{-1} and several others appear below 170 cm^{-1} (70, 130, and 140 cm^{-1}). The absorption lines associated to electronic transitions typically appear between 70 and 140 cm^{-1}. Therefore these lines are on the absorption tail of polar TO-phonon and close to multiphonon transitions. In order to isolate the impurity contribution to the absorption coefficient, two methods were used.

(i) The transmission spectrum of a given sample was divided by that of a reference sample with the same thickness and not exhibiting impurity absorption.

(ii) The transmission spectrum of a given sample was divided by the calculated one corresponding to the polar TO-phonon absorption tail. The absorption coefficient due to multiphonon absorption, as calculated through this method, turns out to be lower than 3 cm^{-1} in the region where the main impurity absorption peaks appear (100–130 cm^{-1}).

Both methods gave the same result when they could be applied to the same sample, the first one providing better spectra, because nearly all of the contribution of the phonon absorption lines was subtracted. After that, line position and line-shape parameters, full width at half maximum (FWHM), and intensity, were obtained using a χ^2 fitting procedure. The test line-shape function has been observed to be Lorentzian. These fitting parameters are listed in Table II.

Typical absorption spectra for samples, from different ingots are shown in Fig. 1–7. In all cases the absorption spectrum is dominated by one or two main lines that are labeled P_n. For high impurity concentration samples, lines at higher (B_n) or lower (A) energy also appear. In samples with faces parallel to the c axis, lines P_n are ob-

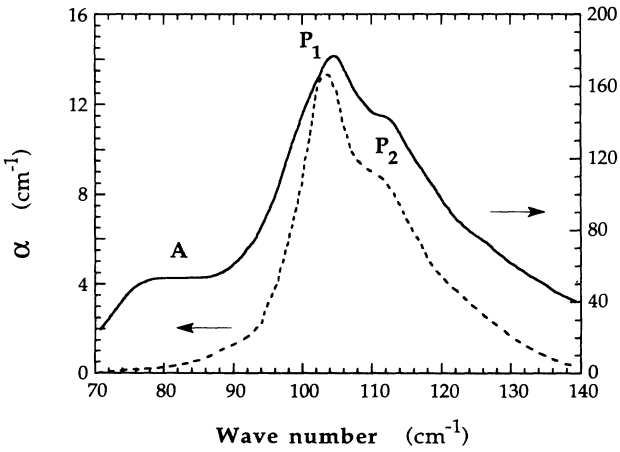

FIG. 2. Impurity absorption coefficient at 5 K for a sample from the SnD-1 ingot, before (dotted line) and after annealing (continuous line).

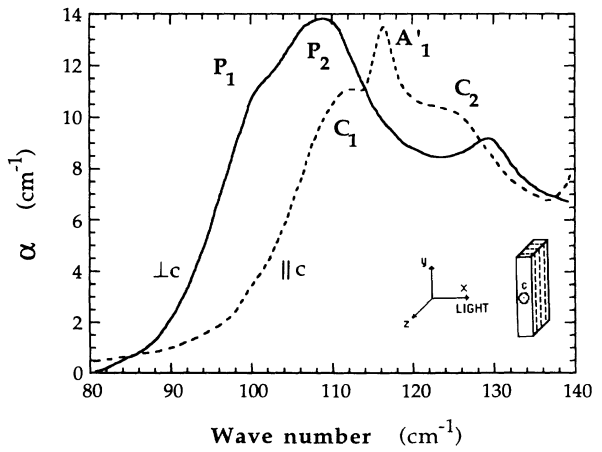

FIG. 4. Impurity absorption coefficient with polarized light at 5 K for a sample cut along the c axis from the SnD-1 ingot.

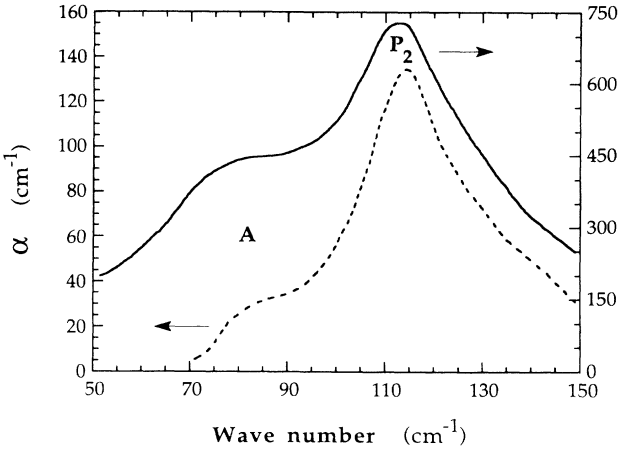

FIG. 5. Impurity absorption coefficient at 5 K for two samples from highly Sn-doped ingots: SnD-3 (dotted line) and SnD-4 (continuous line).

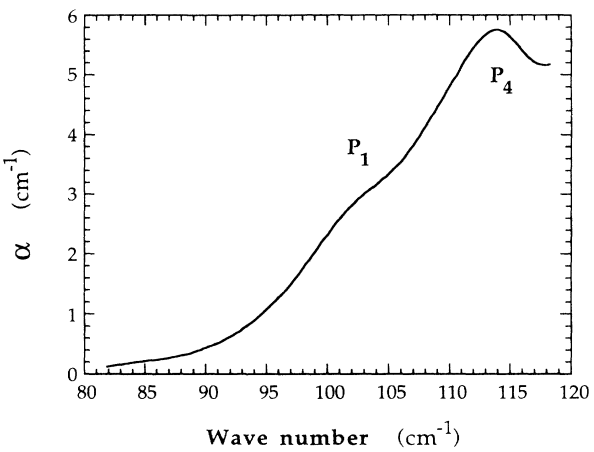

FIG. 7. Impurity absorption coefficient at 5 K in a sample from the Cl-doped ingot.

served for light polarization perpendicular to the c axis, and additional lines (C_n) appear for light polarization parallel to the c axis. Samples from Pb- or Ge-doped ingots do not exhibit any impurity-related absorption peak.

The evolution of FIR spectra as a function of the temperature has been studied for most samples. Figures 8 and 9 show the temperature dependence of the FWHM and integrated intensity of the main lines, P_n, respectively. FWHM increases almost linearly above 20–30 K in all cases, and tends to be constant below 15–20 K. The integrated intensity remains nearly constant up to about 30–40 K, and then decreases with activation energies of about 10 meV, except for the 10% Sn-doped sample whose activation energy is higher than 40 meV.

As regards the line position, temperature shifts are lower than 2 cm^{-1} through the investigated temperature range.

IV. DISCUSSION

The observed absorption lines will be interpreted in the framework of the Guerlach-Pollmann model for uniaxial crystals,[15] applied in our case to electrons bound to impurity atoms, instead of excitons. In this type of crystals, the effective Rydberg energy and Bohr radius are defined by the expressions

$$\mathcal{R}^* = \frac{m_\perp^*}{\epsilon_{0\perp}\epsilon_{0\parallel}}\mathcal{R}_H\ , \qquad a^* = \frac{(\epsilon_{0\perp}\epsilon_{0\parallel})^{1/2}}{m_\perp^*}a_H\ , \tag{1}$$

where $m_\perp^*$ is the electron effective mass perpendicular to the c axis, in units of the free electron mass, and $\epsilon_{0\perp}$ and $\epsilon_{0\parallel}$ are the relative low-frequency dielectric constants, perpendicular and parallel to the c axis, respectively. The

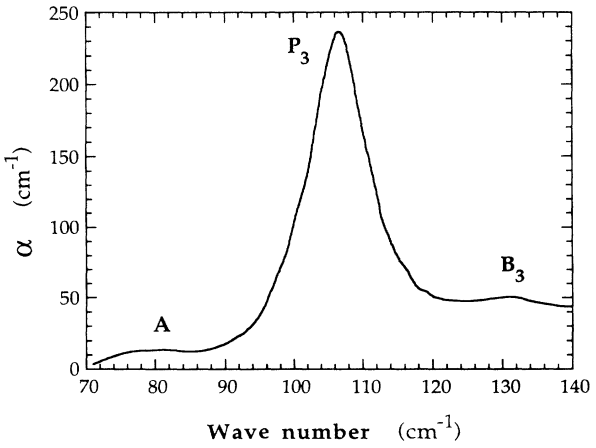

FIG. 6. Impurity absorption coefficient at 10 K for a sample from the Si-doped ingot (SiD).

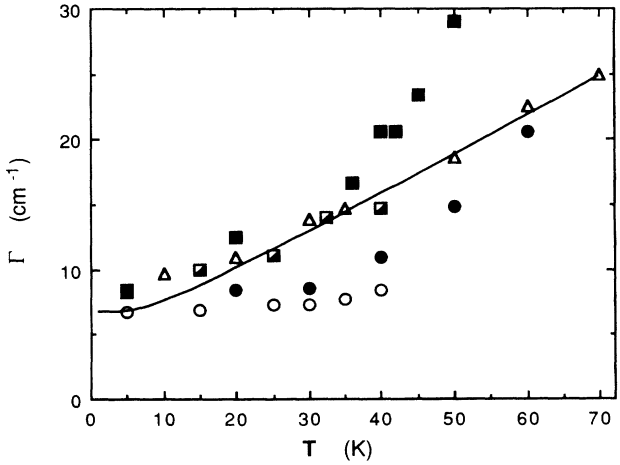

FIG. 8. FWHM of the most representative P_n lines ($1s$-$2p_\pm$ transitions) as a function of the temperature: P_1 line of the ID sample, before (○) and after (●) annealing, P_1 line of the SnD-1 sample (◪), P_2 line of the annealed SnD-2 sample (■), and P_3 line of the SiD sample (△). Full line corresponds to the calculated FWHM through Eq (9), with $\Gamma_0 = 6.6$ cm^{-1} and $T_C = 22$ K.

energies of one-electron states are given by

$$E_{(nl)m}(\alpha)=-\frac{\mathcal{R}^*}{n^2}Z^2_{l|m|}(\alpha)\ , \tag{2}$$

where $Z_{l|m|}(\alpha)$ is the l- and m-dependent effective charge.[15] This magnitude depends on the anistropy parameter α defined as

$$\alpha=1-A\ ,\quad A=\frac{m^*_\perp \epsilon_{0\perp}}{m^*_\parallel \epsilon_{0\parallel}} \tag{3}$$

in which both parallel and perpendicular static dielectric constants and electron effective masses are involved. The effective mass tensor is defined by[12,18]

$$m^*_\perp=0.141\pm0.002\ ,$$

$$m^*_\parallel=0.081\pm0.009\ .$$

The average value of the low-frequency dielectric constants can be obtained from the values reported in the literature[14,19–22] and one gets

$$\epsilon_{0\perp}\epsilon_{0\parallel}=80\pm30\ ,$$

$$\frac{\epsilon_{0\perp}}{\epsilon_{0\parallel}}=1.30\pm0.15\ .$$

The effective Rydberg energy results about 24±9 meV and the anistropy ratio A equal to 23±0.4. The first estimation of the lowest transition energies can be found from Eqs. (2):

$$E_{1s\text{-}2p_\pm}=102\ \text{cm}^{-1}\ ,$$

$$E_{1s\text{-}2p_0}=114\ \text{cm}^{-1}\ ,$$

$$E_{1s\text{-}3p_\pm}=124\ \text{cm}^{-1}\ .$$

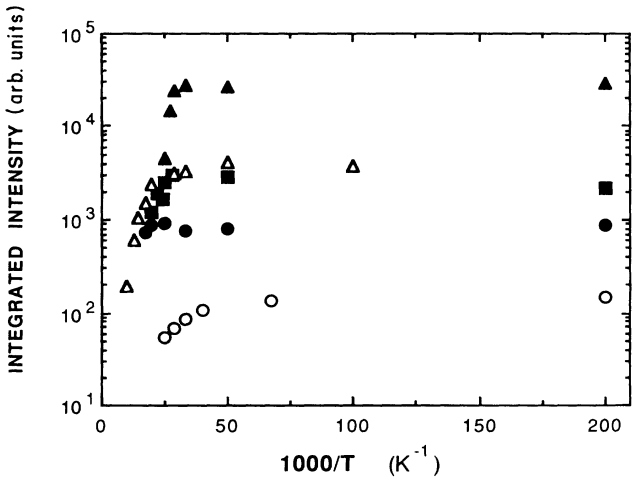

FIG. 9. Integrated intensity of the most representative P_n lines ($1s\text{-}2p_\pm$ transitions) as a function of the temperature: P_1 line of the ID sample, before (○) and after (●) annealing, P_2 line of the annealed SnD-2 sample (■), P_2 line of the SnD-4 sample (▲), and P_3 line of the SiD sample (△).

A. Main absorption lines: transitions from ground state to first excited states

If we compare the experimental energies of lines P_n with the calculated value of $E_{1s\text{-}2p_\pm}$, we can see the coincidence between this transition energy and that of peak P_1. That coincidence suggest that native shallow donors are very hydrogenic, which indicates that the centers responsible for these levels introduce a very weak perturbation in the lattice.

InSe is grown from an initial mixture with indium excess (the proportion was given in the first paragraph of Sec. II), which is segregated to the end of the ingot during the growth. If a little proportion remains in the bulk, the indium atoms could occupy the most stable interstitial positions, which was suggested by Segura *et al.*,[4] in order to explain the origin of the donor level deduced from HE measurements in nondoped samples. Measurements of positron annihilation, reported by De la Cruz *et al.*,[23] are also coherent with this hypothesis. Moreover, Kunc and Zehyer have established,[24] using total energy calculations, that Li($2s^1$) atoms can occupy interstitial positions of equilibrium (minimum energy) in either octahedric or tetrahedric environment. Similarly, In($4s^2p^1$) atoms could be lodged in such positions. When the In atom gets ionized, the perturbation introduced in the lattice is expected to be weak, in view of the spherical symmetry of the In^+ ions, and shallow character would be preserved.

Silicon and tin atoms have an additional electron, compared to In, and chlorine one more than Se. Then, P_2, P_3, and P_4 must also be attributed to the transition $1s\text{-}2p_\pm$ of electrons bound to those shallow donors, with a chemical shift in the ground-state energy of about 3.5, 10, and 11 cm^{-1}, respectively.

The chemical shift observed in substitutional donors depends on the electronegativity and size of these atoms. According to our results, any significant correlation can be established in InSe between these magnitudes. On the other hand, the fact that no absorption lines associated to Ge atoms were observed may be attributed to its high electronegativity. Then, deep levels can be originated if Ge substitutes for In atoms. The largest size of Pb may be the origin of the impossibility that one of these atoms substitutes for only one atom of indium in the lattice. The more likely situation would be the substitution of two atoms of indium by one of lead, yielding a local configuration similar to that of the cation in PbI_2 and $SnSe_2$, which should give rise to an acceptor center.[4] These comments can also be applied to Sn atoms, and a partial compensation can be present in the material. In fact, partial compensation is necessary to account for optical[25] and electrical[10] measurements in Sn-doped samples.

Chemical shift can be accounted for, in a first evaluation (the observed chemical shifts are lower than 10%), by means of a short-range potential included in the effective mass Hamiltonian of Guerlach and Pollmann:[15]

$$H=-\mathcal{R}^*a^{*2}\Delta_r-\frac{2}{r}\mathcal{R}^*a^*f(\alpha,\Theta)-V_0\delta(\mathbf{r}) \tag{4}$$

and using a variational function for the electron ground state:

$$\Psi_{1s}=\left[\frac{Z_{00}^3(\alpha)}{\pi a^{*3}}\right]^{1/2} e^{-(r/a^*)Z_{00}(\alpha)}, \tag{5}$$

where a^*_{var} is the variational parameter. The minimum energy is

$$E_{\min}=\frac{8}{3}\frac{E_0}{\nu^2}\left[\tfrac{3}{2}\nu-1+(1-\nu)^{3/2}\right],$$
$$E_0=-\mathcal{R}^*Z_{00}^2(\alpha), \tag{6}$$

corresponding to a minimum variational parameter

$$a^*_{\text{var}}=\frac{a^*\nu}{2[1-\sqrt{1-\nu}]}, \tag{7}$$

where ν is a magnitude depending on the strength of the central cell potential V_0:

$$\nu=\frac{6V_0Z_{00}(\alpha)}{\pi\mathcal{R}^*a^*}. \tag{8}$$

The variational effective Bohr radii are calculated by Eqs. (6) and (7) for the observed relative energy shifts. These effective radii allow us to calculate the oscillator strengths and relative absorption intensities corresponding to each donor impurity, using expressions that are straightforward, deduced from the Gerlach-Pollmann wave functions.[15] The oscillator strengths for the $1s$-$2p_{\pm}$ transition are 0.343, 0.332, 0.303, and 0.301 for the native, Si-, Sn-, and Cl-related donors, respectively. Using the values of $f_{1s\text{-}2p_{\pm}}$ calculated in that way and the integrated absorption intensity of P_n lines (third column in Table II), we can estimate the neutral donor concentration (lower than the actual impurity concentration if partial compensation exists) in each sample. The result of that calculation is shown in the fourth column of Table II, from which we can observe the large increase of the shallow-donor concentration after a short-time annealing on the samples. This effect is coherent with the model proposed in Ref. 11 and developed in Refs. 9 and 26. In that model, the Bridgman-grown crystals are assumed to consist mainly of the γ polytype, with thin regions (≈ 100 Å in thickness) of the ε polytype, separated by two stacking faults (giving rise to potential barriers) from the bulk γ polytype. The excess In atoms can occupy two different positions in the crystal: (i) isolated interstitial sites in the bulk γ region, where they create shallow donors; and (ii) interstitial sites on the stacking faults: in that perturbed region they produce deep levels.

The annealing process during a short-time interval allows In atoms to diffuse from stacking faults to interstitial sites, which increases the shallow-donor concentration. Afterwards, at room temperature, In atoms are slowly trapped by stacking faults and thus shallow-donor concentration slowly decreases. It has been observed that this relaxation process continues for several days before complete relaxation.[26]

Otherwise, the donor concentration in both nondoped or weakly Sn-doped samples is about 10^{14} cm^{-3}, in contrast to the observed Hall electron concentration at room temperature (see Table I), which is an order of magnitude higher. The mentioned model explains this contradiction, assuming the existence of electrons confined in two-dimensional electric subbands, originated in the interface between stacking faults and the bulk.[9]

Let us now deal with dipole transitions from ground state to higher excited states. The energy differences between P_n and B_n lines ranging from 21 to 24 cm^{-1} (Table II) are very close to the calculated value, between the states $2p_{\pm}$ and $3p_{\pm}$ (22 cm^{-1}). Thus lines B_n are undoubtedly associated to electronic transitions $1s$-$3p_{\pm}$.

Excitation spectra of doped Si and Ge always show the absorption lines corresponding to $1s$-np_0 and $1s$-$np_{\pm}$ transitions. The simultaneous appearance of these lines is due to the existence of several equivalent conduction-band minima at the same point of **k** space. In InSe, only one conduction-band minimum at the Γ point exists and selection rules are satisfied. Effectively, $1s$-$2p_{\pm}$ transitions are allowed when light is polarized perpendicular to the c axis and forbidden in the parallel direction. Therefore C_1 and C_2 absorption lines in Fig. 4, observed when light is polarized parallel to the c axis, must correspond to the transitions $1s$-$2p_0$(In) and $1s$-$2p_0$(Sn), respectively.

Nevertheless, we observe a substantial difference between the calculated (11.6 cm^{-1}) and the experimental quantity $E_{2p_0}-E_{2p_{\pm}}$. This energy is about 30% lower than the calculated one, in the case of In absorption lines (P_1 and C_1), and 15–35% higher, in the case of Sn absorption lines (P_2 and C_2). The homopolar phonon A_1', allowed when light is polarized along the c axis (absorption line at 117 cm^{-1}), could be involved in the origin of this effect. The more likely explanation is a resonant interaction between the bound electrons and this phonon, since the electronic transition energy is near to the phonon energy. Experimental evidences of this type of electron-phonon coupling can be found in silicon,[27–29] and it has been theoretically investigated by Rodriguez and Shultz.[30] The most direct consequence of this resonant interaction is the broadening of that particular absorption line in strictly resonant conditions. When the energies of the electronic transition and optical phonon do not coincide (out of pure resonance), the most outstanding feature is the shifting of the electronic absorption line in a repulsive way, with respect to the phonon frequency.[30] Then, $1s$-$2p_0$ transition would be shifted to lower energies in native donors and to higher energies in tin-related donors, as is actually observed.

At the beginning of this section we pointed out the agreement between experimental transition energies and calculated ones, using the effective mass approximation for uniaxial crystals of Guerlach and Pollmann.[15] However, we have used an average value for the static dielectric constants, which were affected by a large error. Otherwise, we have accurately determined the energies of

$1s$-$2p_{\pm}$ and $1s$-$3p_{\pm}$ transitions associated to native donors, which are the most hydrogenic. Now, we can try to obtain a better estimation of low-frequency dielectric constants from these experimental energies. Expressions (1)–(5) enable us to get

$$A = 2.28 \pm 0.02 ,$$

$$\mathcal{R}^* = 191.8 \pm 1.3 \text{ cm}^{-1} ,$$

which yield

$$\epsilon_{0\perp}\epsilon_{0\parallel} = 80.7 \pm 1.3 ,$$

$$\frac{\epsilon_{0\perp}}{\epsilon_{0\parallel}} = 1.31 \pm 0.15 .$$

The largest relative error on the ratio of dielectric constants arises from the larger error in the electron effective mass parallel to the c axis.

B. Absorption by donor pairs in InSe with high impurity content

The absorption lines labeled as A were observed at lower energy than the others and they did not exhibit any apparent chemical shift. Moreover, their intensities increase with increasing impurity content. These lines must thus be related to an interaction between shallow donors. This phenomenon has been observed and analyzed by Thomas *et al.* in phosphorus-doped silicon,[31] on the basis of hydrogen-molecule-level energies, and assuming a Poisson distribution for the distance between impurities. In this random distribution there exist close pairs of donors, in which energy levels are drastically altered, providing the low-energy transitions.

The ground state of the H_2 molecule, denoted by $^1\Sigma_g^+$, is comprised of the $1s$ states on the two hydrogen atoms. The lowest excited states are denoted by $^1\Sigma_u^+$ and $^1\Pi_u$. The last one corresponds to the state in which one of the electrons comes up to the $2p\pi$ state on the same atom, i.e., $|1s,2p\pi\rangle$ (which has its lobe pointed perpendicular to the axis of separation of the two atoms). The $^1\Sigma_u^+$ state may be represented as a combination of a charge-transfer state $|1s^2,0\rangle$ with both electrons in the $1s$ state on one of the atoms, a state in which an electron is on the $2p\sigma$ state (the lobe is along the axis of separation of the two atoms), i.e., $|1s,2p\sigma\rangle$, and other states of the same symmetry, mainly the $|1s,2s\rangle$ state, as assumed by Kolos and Wolniewicz.[32]

The energies of the first electronic states of the H_2 molecule have been tabulated by Kolos and co-workers[32–34] and, conveniently scaled, can be used to determine the energy levels in donor pairs in our semiconductor. The energies of $1s$, $2p_0$, and $2p_{\pm}$ states of one isolated atom have been corrected by the charge factors $Z_{00}(\alpha)$, $Z_{10}(\alpha)$, and $Z_{11}(\alpha)$, respectively, in order to give account of the uniaxial anistropy in InSe. Figure 10 shows the calculated transition energies between the ground state and the two first excited states in a donor pair, as a function of the distance between donors. The lowest transition energy occurs at about $0.108\mathcal{R}^*$ below the isolated donor transition $1s$-$2p_{\pm}$, and corresponds to the transition from the ground state to the $^1\Sigma_u^+$ state that can be considered, for that distance ($\sim$160 Å), mainly as a charge-transfer (D^+D^-) state. Therefore, if donor concentration is high enough, an absorption line at about 82 cm^{-1} should be expected. Experimentally, A lines are detected at 78–80 cm^{-1}, in correspondence with the previous estimation. The independence of this transition energy with chemical shift can be understood from the larger extension of the electronic system D_2, by comparison to the isolated donor.

It must be pointed out that the pairing between shallow donors is more intense for native donors. The transition to the D^+D^- state is observed in nondoped samples for donor concentrations lower than 10^{15} cm^{-3}, while the donor concentration must be larger that 3–4×10^{15} cm^{-3} in doped samples to obtain a similar intensity (Table II). The origin of this difference could be attributed to the higher mobility of interstitial donors with respect to substitutional donors.

C. Linewidth dependence on the temperature and donor concentration

1. *Temperature dependence: Phonon broadening*

The lowest measured FWHM of the $1s$-$2p_{\pm}$ absorption lines was 6.6 cm^{-1} (sample from the isoelectronic doped ingot) and may be considered as the natural FWHM for this transition in InSe, given the low donor concentration. This condition makes negligible the effects reported in the preceding section and also the influence of internal electric fields, if some compensation was present. Moreover, the line shape for this transition is Lorentzian. The

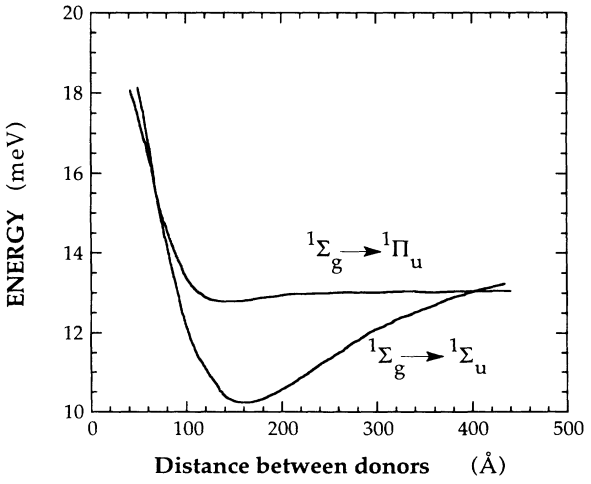

FIG. 10. Transition energies from the ground state to the first two excited ones for a hydrogen like molecule as a function of the interimpurity distance.

interaction between electrons and acoustic phonons would be responsible for the observed natural FWHM and line shape, as occur in Ge or Si.[35,36]

We can use the model proposed by Barrie and Nishikawa in the isotropic case[36] as a rough approximation, taking the following parameters for InSe:[37]

$$\rho = 5.55 \text{ g/cm}^3 ,$$
$$v_s = 2700 \text{ m/s} ,$$
$$\Xi \approx 5 \text{ eV} ,$$

where ρ is the density, v_s the sound velocity along the c axis, and Ξ the deformation potential energy. The FWHM would be about 2 μ eV (mainly due to the coupling between $2p_{\pm}$ and $2s$, $2p_0$ states), nearly three orders of magnitude lower than the experimental value. In spite of this disagreement, the FWHM of P_n transitions in these samples exhibits a temperature dependence close to that coming from the phenomenological expression, deduced by Barrie and Nishikawa for the deformation potential mechanism:[36]

$$\Gamma = \frac{\Gamma_0}{1 - e^{-T_c/T}} , \tag{9}$$

where Γ_0 is the FWHM at 0 K and T_c the characteristic temperature of the electron-phonon interaction. In Fig. 8 the full line fits the low values of the FWHM taking $\Gamma_0 = 6.6 \text{ cm}^{-1}$, and the more typical variation at higher temperature, choosing $T_c = 22$ K. It suggests that the mechanism responsible for the line broadening must be due to some specific feature of longitudinal-acoustic (LA) phonons in layered semiconductors. Recent results on GaSe and InSe have shown that the excitonic Rydberg decreases by 25% in GaSe and 18% in InSe between normal pressure and 2 GPa.[38,39]

Gauthier *et al.* in Ref. 38 propose a model in which that decrease is due to the increase of dielectric constant $\epsilon_{0\parallel}$ under hydrostatic pressure, produced by a charge transfer from the cation-cation bond to interlayer space, which is originated by a fast decrease of the interlayer distance. The dielectric-constant anistropy should disappear when hydrostatic pressure is high enough. Therefore LA phonons, polarized along the c axis, would have generated an associated wave of dielectric constant $\epsilon_{0\parallel}$. This wave would produce a modulation of the effective Rydberg energy of shallow impurities, as well as a modulation of the transition energies between bound states.

This type of LA phonons has an associated pressure wave:

$$|\Delta P| = C_{33} \mathbf{q} \cdot \mathbf{A}_q \exp(i\mathbf{q}\cdot\mathbf{r}) , \tag{10}$$

where C_{33} is the elastic modulus along the c axis and $\mathbf{A}_q$ the amplitude of the acoustic mode. The amplitude of the pressure waves would be

$$P_0 = C_{33} q A_q = C_{33} q \left[\frac{(N_q + \frac{1}{2})\hbar}{2M\omega} \right]^{1/2} ,$$
$$N_q = \left[\exp\left(\frac{\hbar\omega}{k_B T} \right) - 1 \right]^{-1} , \tag{11}$$

where N_q is the occupation number of LA phonons and M the reduced mass of the mode. In the limit $T \to 0$ K,

$$P_0 = C_{33} \left[\frac{\hbar q}{4Mv_s} \right]^{1/2} . \tag{12}$$

The maximum value of q is fixed by the fact that only those LA phonons with wavelength higher than about $2a^*$ can produce a pressure variation in the whole space occupied by the ground state of a shallow impurity. A characteristic energy or temperature can be defined:

$$\hbar\omega = \hbar v_s \frac{\pi}{a^*} ,$$
$$\Theta = \frac{\pi\hbar v_s}{k_B a^*} \tag{13}$$

at which all contributing phonons are excited. This determines the maximum amplitude of the effective pressure waves:

$$P_0 = C_{33} \left[\frac{\pi\hbar}{4Mv_s a^*} \right]^{1/2} = \left[\frac{\pi\hbar C_{33} v_s}{4\Omega a^*} \right]^{1/2} , \tag{14}$$

where Ω is the unit cell volume. Using $a^* = 38$ Å, we get $P_0 = 0.26$ GPa and the ground-state energy would be affected by a modulation about 2.2%, given the linear dependence of the Rydberg energy under pressure up to 2 GPa. This modulation yields an absorption line broadening of about 4.5 cm^{-1}, very close to the observed FWHM.

2. *Concentration dependence: Ionized impurity broadening*

In highly Sn-doped samples (SnD-3 and SnD-4 ingots), the FWHM of P_n absorption lines at low temperature can be as high as 30 cm^{-1}. That value can only be explained through the existence of internal electric fields created by the presence of ionized compensating acceptors. On the other hand, these fields can also be the origin of the large broadening observed for the P_2 line above 40 K (solid squares in Fig. 8) in the annealed SnD-2 sample, more representative than the SnD-1 because line P_2 dominates over P_1.

If the distribution of the ionized impurities, relative to the neutral ones, is completely random, the distribution function of the internal electric fields in the sample is the well-known Holtzmark function.[40,41] The most probable value of the electric field is

$$E_{mH} = 4.16 \frac{e(2N_A)^{2/3}}{4\pi\epsilon} . \tag{15}$$

The absorption line broadening would be of the same

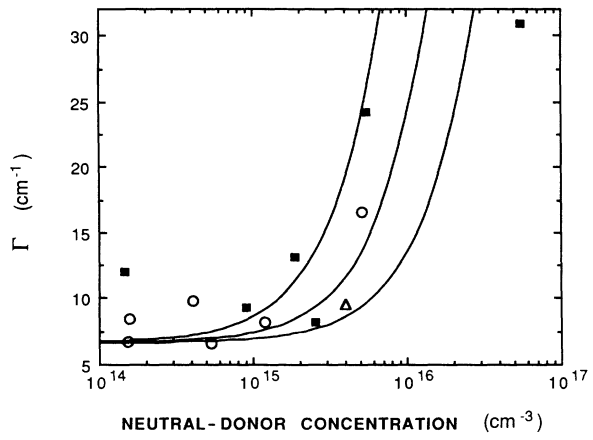

FIG. 11. Variation of FWHM at low temperature as a function of neutral-donor concentration, corresponding to native donors (○), Si- (△) and Sn-related donors (■). Full lines correspond to the FWHM curves, calculated from second-order Stark shift, and assuming a compensation ratio of 5% (curve 1), 10% (curve 2), and 20% (curve 3).

order of the Stark shift, corresponding to that electric field.[41] In uniaxial crystals all the states show second-order Stark effect, because of spatial symmetry, and the theoretical shift is given by[42]

$$\Delta^{(2)}_{(nl)m}(\alpha,\mathcal{E})=2\mathcal{E}^2 a^{*3} Z^2_{00}(\alpha)\frac{m_\perp}{m_\parallel}(\epsilon_\parallel\epsilon_\parallel)^{1/2}h_{(nl)m}(\alpha)\ , \tag{16}$$

where $\mathcal{E}$ is the electric field and $h_{(nl)m}(\alpha)$ is defined as

$$h_{(nl)m}(\alpha)=-\frac{1}{a^{*2}}\sum_{n',l'}\frac{|\langle\varphi_{(n'l')m}(\alpha)|z|\varphi_{(nl)m}(\alpha)\rangle|^2}{[z^2_{lm}(\alpha)/n^2]-[z^2_{l'm'}(\alpha)/n'^2]}\ . \tag{17}$$

Figure 11 shows the dependence of the FWHM for the $1s$-$2p_\pm$ optical transition on neutral donor concentration, calculated by using expressions (15)–(17), for several compensation ratio: 5, 10, 20% and assuming a natural FWHM of 6.6 cm^{-1}. The experimental values for the P_n lines are compatible with that calculation, besides the case of SnD-4 samples, for which the FWHM appears to be lower than the calculated values. That could be attributed to a correlation between the positions of ionized impurities and neutral ones, when increasing the impurity content. Correlation can be taken into account by assuming another distribution function for the internal electric fields, which was deduced by Kogan, Van Lien,[43] and Shklovskii. This distribution probability provides a lower value of the more probable electric field, for the same donor concentration and compensation ratio, and consequently lower broadening.

V. CONCLUSIONS

A systematic study on shallow donors in InSe has been reported. FIR impurity absorption spectra have been interpreted in the framework of the Gerlach-Pollmann model. Electric dipole transitions $1s$-$2p_\pm$, $1s$-$2p_0$, and $1s$-$3p_\pm$, of electrons bound to donor impurities, have been identified through their optical-transition energies and selection rules for polarized light absorption.

Ionization energies of 17.6, 18.1, 18.8, and 19 meV have been determined for the native, silicon, tin, and chlorine donor levels, respectively. Native donors turn out to be the most hydrogenic ones and are proposed to be associated to interstitial In atoms. The other donors are proposed to be substitutional centers in cationic (Si, Sn) or anionic (Cl) positions. Chemical shifts for these donors have also been quantitatively accounted for by including a short-range potential in the electronic Hamiltonian.

The shallow-donor concentration was determined through the calculated oscillator strength of $1s$-$2p_\pm$ transitions. The concentrations of native donors have been shown to increase up to a factor 20 after annealing, coherently with HE previous results. That was interpreted by a model in which excess In atoms, adsorbed to stacking faults (generating deep levels), can diffuse to isolated interstitial sites in the perfect bulk regions (becoming shallow donors) and vice versa.

The product and ratio of low-frequency dielectric constants, perpendicular and parallel to the c axis, were determined from the energies of $1s$-$2p_\pm$ and $1s$-$3p_\pm$ transitions in native shallow donors.

An absorption line associated to donor pairing was observed at about 80 cm^{-1}, independently of the donor type. This transition energy was interpreted through a hydrogenic molecule model, with a rescaling of the energy levels, which takes into account the crystal anisotropy of InSe. The pairing effect was observed to be more intense for interstitial native donors than for substitutional ones.

The FWHM of $1s$-$2p_\pm$ transition in the purest samples (≈ 6.6 cm^{-1}) has been explained by a mechanism, typical of layered semiconductors, in which LA phonons, polarized parallel to the c axis, create a dielectric-constant wave that modulates the electronic binding energies.

The absorption line broadening in highly Sn-doped samples has been explained by the second-order Stark shift, produced by internal electric fields, which are created by ionized compensating acceptors.

ACKNOWLEDGMENTS

This work was supported through Spanish Government CICYT Grant No. MAT90-0242. One of the authors (J.M.-P.) wishes to thank Professor C. Sebenne and Professor M. Balkanski for their hospitality during his stay at the "Laboratoire de Physique des Solides" (Université Paris VI).

[1]R. W. Damon and R. W. Redington, Phys. Rev. **96**, 1498 (1954).
[2]S. M. Atakishiev and G. A. Akhundov, Phys. Status Solidi **32**, K33 (1969).
[3]A. Chevy, Thèse d'état, Université de Paris VI, 1981.
[4]A. Segura, K. Wünstel, and A. Chevy, Appl. Phys. A **31**, 139 (1983).
[5]A. Segura, F. Pomer, A. Cantarero, W. Krause, and A. Chevy, Phys. Rev. B **29**, 5708 (1984)
[6]E. Kress-Rogers, G. F. Hoppert, R. J. Nicholas, W. Hayes, J. C. Portal, and A. Chevy, J. Phys. C **16**, 4285 (1983).
[7]T. Ikari, S. Shigetomi, Y. Koga, and S. Shigetomi, Phys. Status Solidi B **103**, 81 (1981).
[8]Ph. Houdy, Thèse de Troisième Cycle, Université de Paris VII, 1982.
[9]A. Segura, B. Marí, J. Martinez-Pastor, and A. Chevy, Phys. Rev. B **43**, 4953 (1991).
[10]B. Marí, A. Segura, and A. Chevy, Appl. Phys. A **46**, 125 (1988).
[11]B. Marí, A. Segura, A. Cosanovas, and A. Chevy, Appl. Phys. A **52**, 373 (1991).
[12]E. Kress-Rogers, R. J. Nicholas, J. C. Portal, and A. Chevy, Solid State Commun **44**, 379 (1982).
[13]R. Le Toullec, N. Piccioli, and J. C. Chervin, Phys. Rev. B **22**, 6162 (1980).
[14]N. Piccioli, R. Le Toullec, F. Bertrand, and J. C. Bertrand, J. Phys. (Paris) **42**, 1129 (1981).
[15]B. Guerlach and J. Pollmann, Phys. Status Solidi B **67**, 93 (1975).
[16]A. Chevy, J. Cryst. Growth **67**, 119 (1984).
[17]G. L. Belen'kii, L. N. Alieva, R. Kh. Nani, and E. Yu. Salaev, Phys. Status Solidi B **82**, 705 (1977).
[18]R. J. Nicholas, M. A. Brummel, and J. C. Portal, Surf. Sci. **113**, 290 (1982).
[19]J. C. Merle, R. Bartimoro, E Borsella, M. Piacentini, and A. Savoia, Solid State Commun., **28**, 251 (1978).
[20]L. N. Alieva, G. L. Belen'kii, I. I. Reshina, E. Yu. Salaev, and V. Ya. Steinschrieber, Fiz. Tverd. Tela (Leningrad) **21**, 155 (1979) [Sov. Phys. Solid State **21**, 90 (1979)].
[21]K. R. Allakhverdiev, S. S. Babaev, E. Yu. Salaev, and M. M. Tagyev, Phys. Status Solidi B **96**, 177 (1979).
[22]N. Kuroda and Y. Nishina, Solid State Commun. **34**, 481 (1980).
[23]R. M. De la Cruz, R. Pareja, A. Segura, and A. Chevy, J. Phys. C **21**, 4403 (1988).
[24]K. Kunc and R. Zehyer, Europhys. Lett. **7**, 611 (1988).
[25]B. Marí, A. Segura, and A. Chevy, Phys. Status Solidi B **130**, 793 (1985).
[26]J. Martinez-Pastor (unpublished).
[27]A. Onton, P. Fisher, and A. K. Ramdas, Phys. Rev. **163**, 686 (1967).
[28]D. H. Dickey and D. M. Larsen, Phys. Rev. Lett. **20**, 65 (1968).
[29]C. J. Summers, R. B. Dennis, B. S. Wherrett, P. G. Harper, and S. D. Smith, Phys. Rev. **170**, 755 (1968).
[30]S. Rodriguez and T. D. Shultz, Phys. Rev. **178**, 1252 (1969)
[31]G. A. Thomas, M. Capizzi, F. DeRosa, R. N. Bhatt, and T. M. Rice, Phys. Rev. B **23**, 5472 (1981).
[32]W. Kolos and L. Wolniewicz, J. Chem. Phys. **45**, 509 (1966).
[33]W. Kolos and L. Wolniewicz, J. Chem. Phys. **43**, 2429 (1965).
[34]W. Kolos and J. Rychlewski, J. Mol. Spectrosc. **62**, 109 (1976).
[35]K. Nishikawa and R. Barrie, Can. J. Phys. **41**, 1135 (1963).
[36]R. Barrie and K. Nishikawa, Can. J. Phys. **41**, 1823 (1963).
[37]*Zahlenwerte und functionen aus naturwissenschaften und technik,* edited by O. Madelung, Landolt-Börnstein Tables Vol. 17f (Springer-Verlag, Berlin, 1982).
[38]M. Gauthier, A. Polian, J. M. Besson, and A. Chevy, Phys. Rev. B **40**, 3837 (1989).
[39]A. R. Goñi, A. Cantarero, U. Schwarz, K. Syassen, and A. Segura, Bull. Am. Phys. Soc. **35**, 618 (1990).
[40]D. M. Larsen, Phys. Rev. B **13**, 1681 (1976).
[41]Sh. M. Kogan and T. M. Lifshits, Phys. Status Solidi A **39**, 11 (1977).
[42]B. Guerlach and J. Pollmann, Phys. Status Solidi B **67**, 477 (1975).
[43]Sh. M. Kogan, N. Van Lien, and B. I. Shklovskii, Zh. Eksp. Teor. Fiz. **78**, 1933 (1989) [Sov. Phys. JETP **51**, 971 (1980)].